SIAM J. APPL. MATH.
Vol. 61, No. 6, pp. 1839–1856

FOUR-PHASE CHECKERBOARD COMPOSITES*

R. V. CRASTER† AND YU. V. OBNOSOV‡

Abstract. Two-dimensional periodic rectangular checkerboard media are considered in the situation where mean fluxes are prescribed across the structure. The closed-form solution is obtained in the general case where the checkerboard is constructed using four rectangular cells, each having a different, constant resistivity; this four cell structure then repeats doubly periodically to cover the whole plane. This general solution is then used to calculate the effective properties. Thus this four-phase checkerboard encapsulates many limiting and special cases; as a starting point we develop a concise closed-form solution to a basic problem involving four joined quarter planes each of a different resistivity. Subsequent manipulations yield solutions to problems posed in increasingly convoluted domains while retaining the essentially simple structure found for joined quarter planes.

Key words. composite materials, complex analysis, effective parameters

AMS subject classifications. 30E25, 33E05, 73K20, 73V35

PII. S0036139900371825

1. Introduction.

The calculation of effective parameters for composite structures is a topic of wide relevance in many branches of engineering, geology, and physics. Hence there has been a long scientific history associated with the subject, with many different avenues that have been explored. Asymptotic results and theorems for special cases can be found in Bruggeman [5], Keller [14, 15, 16], Dykhne [8], and Mendelson [21]; related to this are recent network resistance analogies, Borcea and Papanicolaou [4] and Borcea [3], and numerical work using integral equations, Gautesen [9]. There are also other numerical schemes, such as, complex power series (Milton, McPhedran, and McKenzie [23]) or other expansion methods (Helsing [10], Hui and Bao [11], and Cheng and Greengard [6]). In addition considerable efforts have been spent on obtaining effective medium approximations or establishing upper and lower bounds for the effective properties (Torquato [29]).

Here we shall concentrate upon one avenue, namely, closed-form solutions to checkerboard composites with the aim of deducing exact formulae for the effective resistivities. This approach is of wide utility because not only do these provide benchmark formulae, but they also yield insight into the underlying mathematical structure; this can be embodied into asymptotic schemes, for instance, for highly differing conductivities; see Keller [16].

Perhaps surprisingly (even for two-phase media) closed-form solutions, and the corresponding formulae for the effective parameters, for this class of problems are not easy to find. There are classical analyses by Rayleigh [28] and Maxwell [20] and much more recent work for square (Berdichevski [2]) or rectangular (Obnosov [26, 27]) checkerboard structures and for biperiodic cylindrical inclusions (Mityushev [24]). Specializing to perfectly conducting or resisting inclusions leads to massive

*Received by the editors May 3, 2000; accepted for publication (in revised form) November 20, 2000; published electronically April 3, 2001.

http://www.siam.org/journals/siap/61-6/37182.html

†Department of Mathematics, Imperial College of Science, Technology and Medicine, London SW7 2BZ, UK (r.craster@ma.ic.ac.uk). The research of this author was supported by an EPSRC Advanced Fellowship.

‡Institute of Mathematics and Mechanics, Kazan State University, University Str., 17, 420008, Kazan, Russia (yurii.obnosov@ksu.ru). The research of this author was supported by Russian Foundation of Basic Research grant N99-01-00364 and the visiting fellowship EPSRC GR/N23288.

simplifications, and then much more progress can be made (Lehner [19] and Kozlov and Vucans [17]).

But beyond this there are few results. It may be that the doubly periodic nature of the boundary value problems has provided an obstacle to further studies; we aim to overcome this here, at least for this specific geometry.

The current paper is, in part, a continuation of the studies by [2, 26, 27], but we introduce the novel concept that much of the analysis can be sidestepped using conformal mappings at an early stage; thus we progress much further and generate solutions for four-phase checkerboard media subjected to a prescribed constant applied field at infinity. Given these solutions we can then evaluate formulae for the effective resistivities, which turn out to have a simple form.

2. Formulation. We consider electrostatic problems in four-phase continuous isotropic linear media whose solution can be represented in terms of a vector field that is both solenoidal and irrotational; in addition to electrostatics this also encompasses several physical scenarios in magneto-statics, heat flow, hydrology, and elasticity. In each phase, distinguished by the subscript k, where $k = 1, \ldots, 4$, we define a vector field $\mathbf{w}_k = (w_{kx}, w_{ky})$ of the horizontal and vertical components w_x, w_y such that both

$$\nabla \cdot \mathbf{w}_k = 0, \qquad \nabla \times \mathbf{w}_k = 0.$$

It is most convenient to utilize complex variables, that is, $z = x + iy$ and $w_k(z) = w_{kx} - iw_{ky}$. In each sector, W_k $(k = 1, \ldots, 4)$, analytic functions $w_k(z)$ are defined. Since we have eigenproblems the results depend crucially upon the singularity behavior at each vertex; from physical considerations these functions have, at most, integrable singularities there. The continuity boundary conditions between each phase are that the normal components of $\mathbf{w}_k$ are continuous across each boundary and that the tangential components of $\rho_k \mathbf{w}_k$ are similarly continuous; the constant parameters ρ_k correspond to a phase property of each medium. For ease of analysis these parameters are taken to be real in the remainder of this paper; this is not a restriction upon the basic method. In the periodic and biperiodic problems we ultimately consider, we take a constant prescribed field at infinity to be the applied forcing.

One could, for instance, take ρ to be the electrical resistivity of a medium; $\rho = 1/\sigma$, with σ as the conductivity. Then taking the vector $\mathbf{w} = \sigma \mathbf{E}$, with $\mathbf{E}$ being the electric field, the usual continuity equations across differing phases leads to the boundary conditions above. We choose to work with the resistivities, rather than the conductivities, for analytic convenience; nonetheless one can rapidly translate our results into effective conductivities if one so requires. We briefly describe the connection with the more conventional notation using the electric field in Appendix C.

3. Analysis. We begin by considering the four joined quarter plane geometry shown in Figure 1, which is the simplest basic geometry consisting of four different phases. In keeping with our earlier complex notation it is clear that we require a solution of the following boundary value problem:

$$\text{Im}[i(\rho_1 w_1 - \rho_2 w_2)] = 0, \quad \text{Im}[w_1 - w_2] = 0 \quad \text{on } 0 < x < \infty, \tag{3.1}$$

$$\text{Im}[i(\rho_4 w_4 - \rho_3 w_3)] = 0, \quad \text{Im}[w_4 - w_3] = 0 \quad \text{on } -\infty < x < 0, \tag{3.2}$$

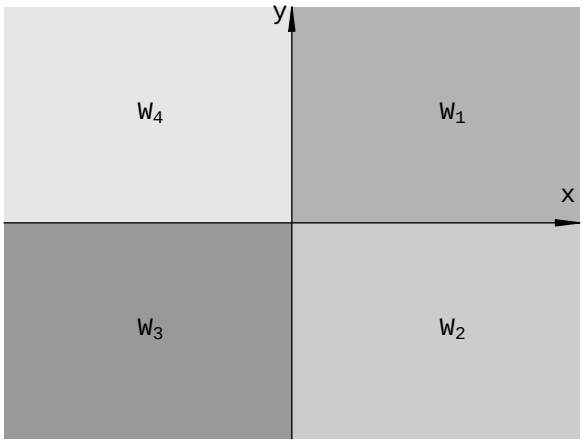

FIG. 1. *Four joined quarter planes each of different resistivity.*

$$\text{Im}[i(w_4 - w_1)] = 0, \quad \text{Im}[\rho_4 w_4 - \rho_1 w_1] = 0 \quad \text{on } 0 < y < \infty, \tag{3.3}$$

$$\text{Im}[i(w_2 - w_3)] = 0, \quad \text{Im}[\rho_2 w_2 - \rho_3 w_3] = 0 \quad \text{on } -\infty < y < 0. \tag{3.4}$$

This can be approached several ways, two of which are discussed in detail in Appendix A; one, using complex variable methods, leads elegantly to a neat formulation, while the other, based upon transform methods, is simpler to apply but yields less elegant results. In either event, the general solution emerges as

$$w_k(\zeta) = \alpha A_k(\lambda)\zeta^{\lambda} + \beta\overline{A_k(\lambda)}\zeta^{-\lambda}, \quad k = 1, \ldots, 4, \tag{3.5}$$

with the $A_k(\lambda)$ defined as

$$\begin{aligned} A_1(\lambda) &= \frac{\rho_2 - \mathrm{i}\,\mathrm{sign}\,\sigma_2\sqrt{\sigma_3/\sigma_1}}{\rho_1 + \rho_2}, \qquad A_2(\lambda) = \frac{\rho_1 - \mathrm{i}\,\mathrm{sign}\,\sigma_2\sqrt{\sigma_3/\sigma_1}}{\rho_1 + \rho_2}, \\ A_3(\lambda) &= \mathrm{e}^{\mathrm{i}\,\pi\lambda}\left[\frac{\rho_4 - \mathrm{i}\,\mathrm{sign}\,\sigma_2\sqrt{\sigma_3/\sigma_1}}{\rho_3 + \rho_4}\right], \quad A_4(\lambda) = \mathrm{e}^{-\mathrm{i}\,\pi\lambda}\left[\frac{\rho_3 - \mathrm{i}\,\mathrm{sign}\,\sigma_2\sqrt{\sigma_3/\sigma_1}}{\rho_3 + \rho_4}\right]. \end{aligned} \tag{3.6}$$

As it stands these are eigensolutions that are chosen to have integrable singularities at the origin. In subsequent sections the real constants α and β are to be determined in each physical example from prescribed applied mean fluxes across the four cells or four semi-infinite strips. These solutions contain several parameters that we give here:

$$\sigma_1 = \rho_1 + \rho_2 + \rho_3 + \rho_4, \quad \sigma_2 = \rho_1\rho_3 - \rho_2\rho_4, \tag{3.7}$$

$$\sigma_3 = \rho_1\rho_2\rho_3 + \rho_1\rho_2\rho_4 + \rho_1\rho_3\rho_4 + \rho_2\rho_3\rho_4, \tag{3.8}$$

$$\cos\pi\lambda = 1 - 2\Delta^2, \quad \Delta^2 = \frac{\sigma_2^2}{\sigma_1\sigma_3 + \sigma_2^2}. \tag{3.9}$$

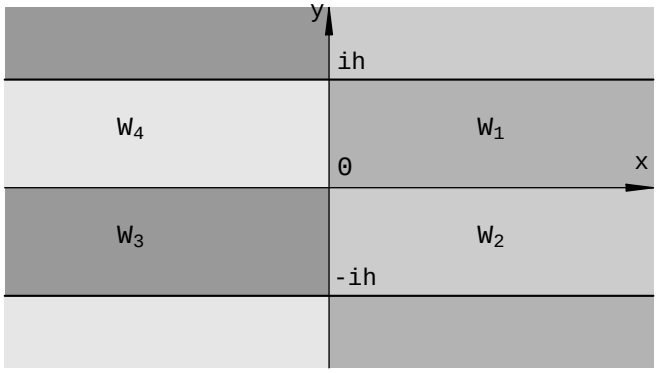

FIG. 2. *The geometry for a periodic four-phase system of four semi-infinite strips in the physical, z, plane.*

For any reader referring back to earlier papers, say, [26], we should note that our present definition of λ is twice that as used there and differs from it in sign σ_2. The full details regarding how these parameters emerge from the analysis is contained in Appendix A. This solution is vital to the following sections; we shall conformally map more geometrically involved domains into this and/or take advantage of the simple structure we have found.

4. Periodic media. As an initial step we shall consider singly periodic media where we have four semi-infinite strips each of vertical height h that periodically repeat; this is shown schematically in Figure 2.

To utilize the four joined quarter plane solution given above, it is necessary to conformally map this semi-infinite arrangement into the four quarter planes while ensuring that all the continuity conditions and the periodicity are maintained. The mapping $\zeta(z) = \tanh(\pi z/2h)$ does precisely this by mapping the points which were at $\pm\infty$ in the physical plane to ± 1 in the ζ plane; the function is clearly periodic. The continuity boundary conditions are important; clearly along the paths from 0 to $\pm\infty$ and from 0 to $\pm ih$ we require the periodicity conditions to hold, and the mapping places these along the real or imaginary axes such that the solution derived for four joined quarter planes deals correctly with this issue. For the solution to be periodic with the continuity conditions holding along the lines $\pm ih$ to $\pm ih \pm \infty$, we also require these lines to be mapped to adjoining pieces of the real axis; this is also done by this mapping.

One could avoid this conformal mapping argument by asking oneself to determine the periodic function such that the horizontal boundaries of the strips map to adjoining sections of the real axis and vertical boundaries to the imaginary axis; the only functions to do this are $\tanh(\pi z/2h)$ and of course its inverse $\coth(\pi z/2h)$. The inverse also appears naturally as we have $\zeta^{\pm\lambda}$ in the basic quarter plane solution.

Thus in the ζ plane we recover precisely the four quarter plane solution, (3.5), but with $\zeta(z)$ as the tanh function; hence we can directly utilize our solution to the four joined quarter planes.

The real constants α, β which appear in the solution (3.5) must now be determined using given flux conditions. That is, the mean fluxes a and b through the sides of

each periodic arrangement are given as

$$a = \frac{1}{2h}\int_{-h}^{h} \mathrm{Re}[w_k(0,y)]dy, \quad b = \frac{1}{2l}\int_{-l}^{l} \mathrm{Im}[w_k(x,0)]dx \quad \text{as} \quad l \to \infty. \tag{4.1}$$

Given these mean fluxes we then need to relate these to the constants α and β that appear in (3.5). The integrals in (4.1) can be done explicitly using the results in Appendix B, and it is found that

$$a = \frac{(\alpha+\beta)}{2}, \quad b = -\frac{(\alpha-\beta)}{2}\mathrm{sign}\,(\sigma_2)\sqrt{\sigma_3/\sigma_1}\frac{(\rho_3+\rho_4+\rho_1+\rho_2)}{(\rho_1+\rho_2)(\rho_3+\rho_4)}, \tag{4.2}$$

and thus we can determine α and β as

$$a \pm b\frac{\mathrm{sign}\,\sigma_2}{(\sigma_1\sigma_3)^{\frac{1}{2}}}(\rho_1+\rho_2)(\rho_3+\rho_4)$$

with α taking the negative sign and β the positive.

It is convenient to evaluate each vertical and horizontal integral along the axes, and there is no loss of generality in doing so. The subscript k takes the appropriate value depending on which phase we are in, and w_k has the arguments (x, y) associated with the physical problem.

We are now in a position to be able to calculate some effective parameters. The effective resistivities (these are the reciprocal of the conductivities) along the x and y axes are

$$\rho_y = \frac{1}{2hb}\int_{-h}^{h} \mathrm{Im}[\rho_k w_k(0,y)]dy, \tag{4.3}$$

$$\rho_x = \frac{1}{2la}\int_{-l}^{l} \mathrm{Re}[\rho_k w_k(x,0)]dx \quad \text{as } l \to \infty. \tag{4.4}$$

Evaluating these integrals (see Appendix B) one finds that

$$\rho_x = \frac{\rho_1\rho_2}{(\rho_1+\rho_2)} + \frac{\rho_3\rho_4}{(\rho_3+\rho_4)}, \quad \rho_y = \frac{(\rho_3+\rho_4)(\rho_1+\rho_2)}{(\rho_1+\rho_2+\rho_3+\rho_4)}. \tag{4.5}$$

Other effective parameters, such as an effective resistivity tensor, can be deduced. In the complex notation we evaluate

$$\rho = \int_W \rho_k w_k(z)dA \Big/ \int_W w_k(z)dA. \tag{4.6}$$

It turns out that

$$\rho \equiv \left(\frac{a\rho_x - ib\rho_y}{a-ib}\right), \tag{4.7}$$

with $W = \sum_k W_k$, and ρ_k, w_k take their respective values in each W_k. That is, we in some sense average over the area of the four strips. The resulting complex ρ is $\rho = \rho_{xx} - i\rho_{xy} = \rho_{yy} + i\rho_{yx}$, where ρ_{ij} are the components of an effective resistivity tensor.

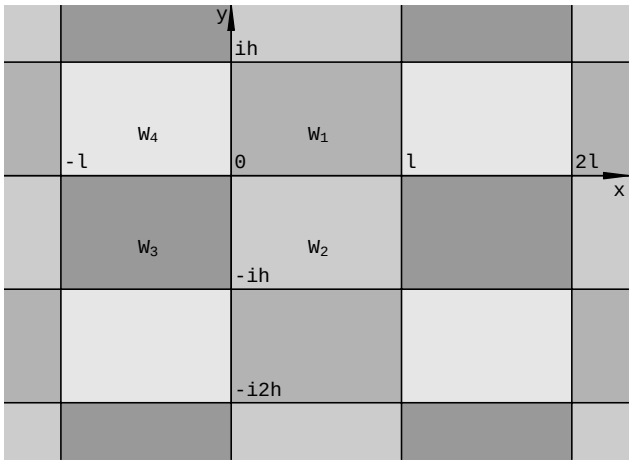

FIG. 3. *The geometry for a doubly periodic four-phase checkerboard in the physical plane.*

The effective energy dissipation is

$$D = \frac{1}{4lh}\int_W \rho_k |w_k(z)|^2 dA = a^2\rho_x + b^2\rho_y. \tag{4.8}$$

Many special and limiting cases can be deduced from these, and the formulae for ρ and D are also valid for the doubly periodic domains, but we shall not dwell upon the special cases for the periodic geometry here.

5. Doubly periodic. The situation that we now face is a doubly periodic checkerboard of four cells, each potentially a different phase; a schematic is shown in Figure 3. The individual cells, the W_j, have width l and height h. Perhaps surprisingly there is also a function in this geometry that behaves just as the hyperbolic tangent did for singly periodic media; not surprisingly it involves Jacobi elliptic functions which are themselves doubly periodic.

For periodic media we asked ourselves to determine a singly periodic function mapping horizontal boundaries to adjoining segments of the real axis in the ζ plane, so that continuity at the top and bottom of each cell was maintained. Now we search for a doubly periodic function that, in addition, maps the vertical boundaries to the imaginary axis in the ζ plane; thus we again have the basic four quarter plane solution, but now with ζ replaced by this function. It is found that

$$\zeta(z) = \left[\frac{1 - \mathrm{cn}\left(\frac{2K(m)z}{l}|m\right)}{1 + \mathrm{cn}\left(\frac{2K(m)z}{l}|m\right)}\right]^{\frac{1}{2}} \tag{5.1}$$

is the required function; the cn are the Jacobi elliptic cosinus functions; see, for instance, Lawden [18]. An alternative argument based upon conformal mappings appears in Craster [7]; formally one can map the rectangular region consisting of four cells into a four quarter plane structure using the elliptic sinus

$$\mathrm{sn}\left(\frac{K(m)z}{l}|m\right).$$

But importantly this does not map the vertical boundaries correctly, and a further manipulation of this is required that leads to (5.1). One noteworthy feature of this mapping is that we get a two-sheeted Riemann surface, but the continuity conditions are still satisfied correctly as formal substitution into the final form will readily reveal. Also appearing in this formula are the complete elliptic integral of the first kind, $K(m)$, and the parameter m. This parameter is implicitly defined via $K(m)/K(1-m) = l/h$ and explicitly builds the aspect ratio of each cell into the analysis. Note that $m = 1$ is the limit where we recover the semi-infinite strips, and the tanh function naturally reemerges. The really noteworthy point is that the complicated Markushevich approach utilized in earlier papers is not required.

It is also worthwhile noting that one can obtain accurate asymptotic representations for m as

$$m \sim \begin{cases} 16\exp(-\pi h/l) & \text{for} \quad h \gg l \\ 1 - 16\exp(-\pi l/h) & \text{for} \quad h \ll l, \end{cases} \tag{5.2}$$

and these are useful in geometries with large aspect ratio.

To fully determine the solution (3.5) we need α and β. To find these we prescribe the mean fluxes through the four cells, a and b, which are defined using

$$a = \frac{1}{2h}\int_{-h}^{h} \mathrm{Re}[w_k(0,y)]dy, \quad b = \frac{1}{2l}\int_{-l}^{l} \mathrm{Im}[w_k(x,0)]dx. \tag{5.3}$$

These integrals are evaluated using results from Appendix B as

$$a = \frac{(\alpha+\beta)}{2\sigma(1-m)}, \tag{5.4}$$

and

$$b = -\frac{(\alpha-\beta)}{2\sigma(m)\cos\frac{\pi\lambda}{2}}\mathrm{sign}\,(\sigma_2)\sqrt{\sigma_3/\sigma_1}\left[\frac{(\rho_3+\rho_4+\rho_1+\rho_2)}{(\rho_1+\rho_2)(\rho_3+\rho_4)}\right]. \tag{5.5}$$

Solving these we finally obtain α, β as

$$a\sigma(1-m) \pm b\sigma(m)\mathrm{sign}\,\sigma_2\left[\frac{(\rho_1+\rho_2)(\rho_3+\rho_4)}{(\rho_1+\rho_4)(\rho_2+\rho_3)}\right]^{\frac{1}{2}},$$

with α taking the negative sign and β the positive.

An important parameter in these formulae is $\sigma(m)$ defined as

$$\sigma(m) = \frac{\frac{2}{\pi}K(m)}{P_{\frac{\lambda}{2}-\frac{1}{2}}(1-2m)}; \tag{5.6}$$

also appearing are the Legendre function of the first kind $P_\nu(1-2m)$, and $K(m)$ is the elliptic integral discussed earlier. The ratio $\sigma(m)/\sigma(1-m)$ is ubiquitous in the expressions associated with effective parameters and is

$$\frac{\sigma(m)}{\sigma(1-m)} = \frac{l}{h}\frac{P_{\frac{\lambda}{2}-\frac{1}{2}}(2m-1)}{P_{\frac{\lambda}{2}-\frac{1}{2}}(1-2m)}; \tag{5.7}$$

the geometric dependence is encapsulated in the l/h terms and, of course, in m, and the material dependence in each phase is encapsulated in λ.

It is perhaps noteworthy that there are two special angles of the flux for which the solution defined via (3.5), (3.6), (5.1) has singularities at two diagonal off vertices of each phase W_k and vanishes at two others.

Now that we have the full solution, w_k, we can determine the effective parameters from the integrals

$$\rho_y = \frac{1}{2hb}\int_{-h}^{h} \mathrm{Im}[\rho_k w_k(0,y)]dy \quad \text{and } \rho_x = \frac{1}{2la}\int_{-l}^{l} \mathrm{Re}[\rho_k w_k(x,0)]dx, \tag{5.8}$$

and, after some effort, and using results from Appendix B, the following forms emerge:

$$\rho_x = \frac{\sigma(1-m)}{\sigma(m)}\left[\frac{(\rho_2+\rho_3)(\rho_4+\rho_1)}{(\rho_1+\rho_2)(\rho_3+\rho_4)}\right]^{\frac{1}{2}}\left(\frac{\sigma_3}{\sigma_1}\right)^{\frac{1}{2}}, \tag{5.9}$$

$$\rho_y = \frac{\sigma(m)}{\sigma(1-m)}\left[\frac{(\rho_1+\rho_2)(\rho_3+\rho_4)}{(\rho_2+\rho_3)(\rho_4+\rho_1)}\right]^{\frac{1}{2}}\left(\frac{\sigma_3}{\sigma_1}\right)^{\frac{1}{2}}. \tag{5.10}$$

Apart from the relative simplicity of these formulae, there are a couple of noteworthy features, the first being that rotating the four-cell structure through a right angle and appropriately renumbering the phases allows one to deduce ρ_x from ρ_y and vice versa. Secondly there is a simple relation for their product, that is, $\rho_x\rho_y = \sigma_3/\sigma_1$, and this should be useful in any numerical work. The results for ρ and D follow from those in (4.7), (4.8), (5.9), (5.10).

Given that our final solution for the w_k contains an implicit definition for m together with Jacobi elliptic functions, and our resistivity formulae also contain m and Legendre functions, one might query whether these are numerically awkward to evaluate. The value of m is rapidly found using standard root-finding algorithms, and the special functions are defined in symbolic manipulation packages such as Mathematica, or alternatively they all have integral representations that can be evaluated using Gaussian quadrature. Some example numerical evaluations for two and three phases can be found in [7, 27] and in [13].

5.1. Special cases. There are numerous special cases that can be of interest, and we shall present the results of some of them here. These fall into two classes: geometrical special cases—square checkerboards with $h = l$, cells of large aspect ratio—and those with some phases equal.

5.1.1. Symmetry about one diagonal: $\boldsymbol{\rho_2 \equiv \rho_4}$. This special case maintains some symmetry, namely, in each four-cell grouping about $y/h = x/l$; see Figure 4. If, furthermore, $\rho_1 = \rho_3$, we have a chessboard structure as recently analyzed by Obnosov [26], for which

$$\rho_x = \frac{\sigma(1-m)}{\sigma(m)}\sqrt{\rho_1\rho_2}, \quad \rho_y = \frac{\sigma(m)}{\sigma(1-m)}\sqrt{\rho_1\rho_2}. \tag{5.11}$$

This rectangular checkerboard is the most often studied arrangement, and several useful theorems (Keller [15], Mendelson [21], and Dykhne [8]) and numerical results (Gautesen [9]) have appeared for it.

If $\rho_1 = \rho_2 = \rho_4$, then we have isolated rectangular inclusions, also recently studied by Obnosov [27], and then

$$\rho_x = \frac{\sigma(1-m)}{\sigma(m)}\rho_1\sqrt{\frac{\rho_1+3\rho_3}{\rho_3+3\rho_1}}, \quad \rho_y = \frac{\sigma(m)}{\sigma(1-m)}\rho_1\sqrt{\frac{\rho_1+3\rho_3}{\rho_3+3\rho_1}}. \tag{5.12}$$

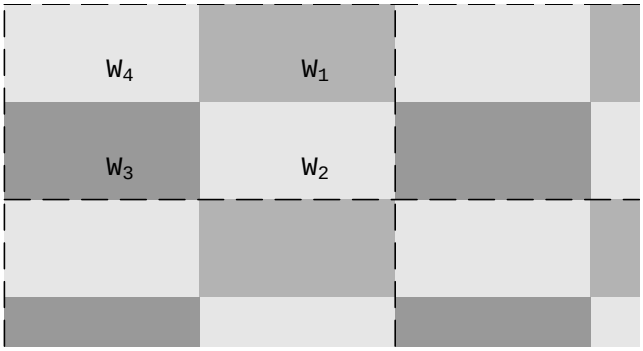

FIG. 4. *Symmetry about one diagonal.*

Our analysis in the present paper departs from that in [26, 27] at a crucial point, that is, we do not tackle the formidable Markushevich conjugate Riemann boundary value problems in the doubly periodic domain; we avoid this by utilizing conformal mappings directly. This latter approach is advocated in [7], but that paper is limited in that it concentrates only upon $\rho_2 = \rho_4$, as the pleasant form of the basic four joined quarter plane solution presented here in Appendix A was, at that time, not forthcoming. Thus those results are restricted, and for $\rho_2 = \rho_4$ one has that

$$\rho_x = \frac{\sigma(1-m)}{\sigma(m)} \left(\frac{\rho_1[\rho_1\rho_3 + \rho_1\rho_2 + \rho_1\rho_3 + \rho_2\rho_3]}{\rho_1 + 2\rho_2 + \rho_3} \right)^{\frac{1}{2}},$$

$$\rho_y = \frac{\sigma(m)}{\sigma(1-m)} \left(\frac{\rho_1[\rho_1\rho_3 + \rho_1\rho_2 + \rho_1\rho_3 + \rho_2\rho_3]}{\rho_1 + 2\rho_2 + \rho_3} \right)^{\frac{1}{2}}; \tag{5.13}$$

these do not highlight the remarkably simple and elegant forms of the general representations in (5.9), (5.10). All of these formulae have ρ_x and ρ_y identical, except for the $\sigma(1-m)/\sigma(m)$ terms, and this must be so as rotation of the basic four-cell structure through a right angle indicates. Each of these special cases can be further specialized to allow one or, in the later case, two phases to be perfectly resistive or conducting, that is, $\rho = 0, \infty$ and further simplifications ensue.

5.1.2. Two equal neighboring phases: $\boldsymbol{\rho_1 = \rho_4}$. Thus we now have three phases, one of which becomes an infinite strip of height h, whereas the remaining phases retain their block structure; this is shown in Figure 5. Here

$$\rho_x = \frac{\sigma(1-m)}{\sigma(m)} \rho_1 \left(\frac{2[\rho_2 + \rho_3][\rho_1\rho_2 + \rho_1\rho_3 + 2\rho_2\rho_3]}{[\rho_1 + \rho_2][\rho_3 + \rho_1][2\rho_1 + \rho_2 + \rho_3]} \right)^{\frac{1}{2}},$$

$$\rho_y = \frac{\sigma(m)}{\sigma(1-m)} \left(\frac{[\rho_1 + \rho_2][\rho_3 + \rho_1][\rho_1\rho_2 + \rho_1\rho_3 + 2\rho_2\rho_3]}{2[\rho_2 + \rho_3][2\rho_1 + \rho_2 + \rho_3]} \right)^{\frac{1}{2}}. \tag{5.14}$$

Notably we have lost the simple rotational symmetry evident in the preceding section. A useful further limiting case is to allow $\rho_2 = \rho_3$ so that we recover a trivial situation of alternating strips; this situation also arises in the next section, and we discuss it there.

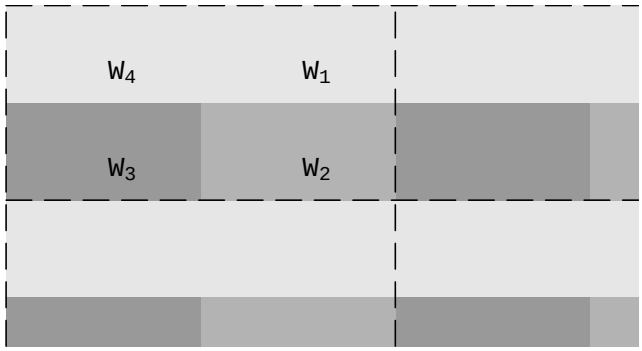

FIG. 5. *Two equal neighboring phases.*

5.1.3. Aspect ratio independence: $\rho_1\rho_3 = \rho_2\rho_4$. At first sight it is not clear what this case physically means, and it does not arise in section 5.1.1 except as a completely degenerate trivial case, that is, $\rho_k = \rho_1$ for $k = 1, \ldots, 4$. Nonetheless it is an interesting subcase as now $\lambda = 0$ and the term $\sigma(1-m)/\sigma(m) = 1$; hence the dimensions h and l play no role in ρ_x, ρ_y. Thus

$$\rho_x = \rho_1 \frac{(\rho_2 + \rho_3)}{(\rho_1 + \rho_2)}, \quad \rho_y = \rho_3 \frac{(\rho_1 + \rho_2)}{(\rho_2 + \rho_3)}. \tag{5.15}$$

It is noteworthy that $\rho_x\rho_y = \rho_1\rho_3 = \rho_2\rho_4$.

A further case of this is when $\rho_1 = \rho_4$ and $\rho_2 = \rho_3$; this doubly periodic example now coincides with a simple arrangement of periodic alternating strips whose effective resistivities are trivially

$$\rho_x = \frac{2\rho_1\rho_2}{(\rho_1 + \rho_2)}, \quad \rho_y = \frac{(\rho_1 + \rho_2)}{2}. \tag{5.16}$$

Similarly $\rho_1 = \rho_2$ and $\rho_3 = \rho_4$ leads to

$$\rho_x = \frac{(\rho_1 + \rho_3)}{2}, \quad \rho_y = \frac{2\rho_1\rho_3}{(\rho_1 + \rho_3)}; \tag{5.17}$$

it is reassuring to recover these limiting results from our full analysis. In general, though, it is interesting to note that there are these additional nontrivial arrangements of phase combinations with $\rho_1\rho_3 = \rho_2\rho_4$ that lead to effective parameters independent of the aspect ratio; this independence can also be deduced using [12].

5.1.4. Highly contrasting phases. If two of the phases along the diagonal of each four-cell structure are considerably larger than the others, say, $\rho_1, \rho_3 \gg \rho_2, \rho_4$, then $\Delta \sim 1, \lambda \sim 1$ and hence the crucial ratio $\sigma(1-m)/\sigma(m) \sim l/h$, and one simply obtains

$$\rho_x \sim \frac{l}{h}\left[\frac{\rho_1\rho_3(\rho_2 + \rho_4)}{(\rho_1 + \rho_3)}\right]^{\frac{1}{2}}, \quad \rho_y \sim \frac{h}{l}\left[\frac{\rho_1\rho_3(\rho_2 + \rho_4)}{(\rho_1 + \rho_3)}\right]^{\frac{1}{2}}. \tag{5.18}$$

If we have a two-phase medium with $\rho_1 = \rho_3$, $\rho_2 = \rho_4$, then the analogous limiting value also emerges from the numerical and asymptotic approaches of Gautesen [9] and also Keller [16]. Formulae found in this high-contrast limit also have the added advantage that they can be used in three-dimensional asymptotic studies for four-phase

cubes in a similar manner to that advocated in [16]. Effective properties for composites consisting of highly contrasting phases are awkward to evaluate numerically [11], and these results should be valuable checks upon such studies.

5.1.5. Square checkerboards. So far we have concentrated upon rectangular cells of arbitrary aspect ratio; if we specialize to $h \equiv l$, that is, square cells, then $m = 1/2$ and the ratio $\sigma(1-m)/\sigma(m) = 1$. Thus

$$\rho_x = \left[\frac{(\rho_2+\rho_3)(\rho_4+\rho_1)}{(\rho_1+\rho_2)(\rho_3+\rho_4)}\right]^{\frac{1}{2}} \left(\frac{\sigma_3}{\sigma_1}\right)^{\frac{1}{2}}, \tag{5.19}$$

$$\rho_y = \left[\frac{(\rho_1+\rho_2)(\rho_3+\rho_4)}{(\rho_2+\rho_3)(\rho_4+\rho_1)}\right]^{\frac{1}{2}} \left(\frac{\sigma_3}{\sigma_1}\right)^{\frac{1}{2}}, \tag{5.20}$$

and these provide the generalization of the classical Dykhne [8] formulae to four-phase checkerboard composites; this four-phase result is conjectured in Mortola and Steffé [25].

5.1.6. High aspect ratio asymptotics. As noted earlier there are nice asymptotic formulae for the critical parameter m when either $h \gg l$ or $h \ll l$, (5.2); thus we can determine the ratio $\sigma(m)/\sigma(1-m)$ as

$$\frac{\sigma(m)}{\sigma(1-m)} \sim \cos(\pi\lambda/2)\left[1 - \frac{l}{\pi h}\left(2\gamma + 2\psi\left(\frac{1}{2}+\frac{\lambda}{2}\right) + \pi\cot\left[\pi\left(\frac{1}{2}+\frac{\lambda}{2}\right)\right] + 4\log 2\right)\right] \tag{5.21}$$

for $h \gg l$. Thus asymptotic representations of the effective parameters can be determined as, for instance,

$$\rho_x \sim \frac{(\rho_1+\rho_4)(\rho_2+\rho_3)}{(\rho_1+\rho_2+\rho_3+\rho_4)}\left[1 - \frac{l}{\pi h}\left(2\gamma + 2\psi\left(\frac{1}{2}+\frac{\lambda}{2}\right) + \pi\cot\left[\pi\left(\frac{1}{2}+\frac{\lambda}{2}\right)\right] + 4\log 2\right)\right]^{-1}$$

$$+ O(\exp(-\pi h/l)) \qquad \text{for} \quad h \gg l. \tag{5.22}$$

In (5.22) the parameter γ is Euler's constant and ψ is the Psi function defined in the usual manner (Abramowitz and Stegun [1]). Similarly if $h \ll l$, one finds that

$$\rho_x \sim \left[\frac{\rho_1\rho_2}{(\rho_1+\rho_2)} + \frac{\rho_3\rho_4}{(\rho_3+\rho_4)}\right]\left[1 - \frac{h}{\pi l}\left(2\gamma + 2\psi\left(\frac{1}{2}+\frac{\lambda}{2}\right) + \pi\cot\left[\pi\left(\frac{1}{2}+\frac{\lambda}{2}\right)\right] + 4\log 2\right)\right]$$

$$+ O(\exp(-\pi l/h)) \qquad \text{for} \quad h \ll l. \tag{5.23}$$

It is evident that in the appropriate limits we recover those found in section 4. One additional noteworthy feature, after inspecting higher terms, of these formulae is that for a four-cell structure $2l \times 2h$ these provide upper and lower bounds upon ρ_x; importantly these are not just the crude bounds we would get from using the semi-infinite strip results but build in the geometric dependence. Similar results are found for ρ_y; these results are surprisingly accurate over a wide range of h and l; a numerical example appears in [7].

6. Concluding remarks. The underlying idea that we present here is that one can begin with a conceptually simple situation, four joined quarter planes, and that subsequent manipulations of this lead us to the solution of much harder geometries from which we can then deduce the effective resistivities. In particular we have concentrated upon rectangular checkerboard media which, for two phases, have been a much studied model geometry. As demonstrated here, formulae for the effective parameters can be deduced that incorporate explicitly the geometrical and phase dependence. The final formulae for the effective resistivities along the axes (5.9), (5.10) are surprisingly simple in structure and encompass many special and limiting cases; these provide valuable benchmarks for any numerical or future analytical studies.

Many special cases occur, some limiting cases where we recover known results, and also others; for instance, we identify a limit whereby four phases exist, but the effective resistivities are geometrically independent. It is also shown how results for the checkerboard can be used to recover those for long thin alternating strips of material.

It is perhaps worthwhile comparing our approach with those numerical schemes for checkerboard geometries that are based upon series expansions using eigensolutions for four joined quarter planes. Thus far these calculations have been for two phases (see, for instance, [10]), although they also include parallelogram as well as rectangular checkerboards, and are based upon the results deduced by Keller [16]. They use an infinite series representation with an infinite number of eigenvalues, whereas we have used two eigenvalues $\pm\lambda$. That our solution involves merely two eigenvalues is due to the constraint of having integrable singularities at each vertex while we simultaneously satisfy both continuity conditions on the lines emanating from the vertex and periodicity at the edges of each cell. The series approach also has the physical constraint, but the quarter plane eigensolutions do not satisfy the continuity and periodicity conditions at the edges of the four-cell checkerboard structure, and thus an expansion together with simultaneous equations is required. The mapping procedure we use here sidesteps this, and we have, in effect, managed to sum the series that these numerical methods produce.

The effective resistivity formulae we have deduced are the first rigorous closed-form results to be deduced for four-phase model composites. As such they confirm conjectures in Mortola and Steffé [25] regarding the form of the effective parameters for square checkerboards and relations between the parameters for rectangular checkerboards; very recently their conjectures have independently been proved to be correct by Milton [22] using different methods. It is envisaged that the formulae deduced herein will not only be useful as benchmarks, but will also provide elementary bounds on parameters and in further asymptotic studies.

Appendix A. The solution for four joined quarter planes. A simple, and importantly also concise, closed-form solution of the basic four quarter plane problem is essential for use in the text. There are two main approaches; first we use complex variables directly, which turns out to be more technically involved, but ultimately leads directly to a simple solution. Alternatively one can adopt a transform-based approach which for some simpler limiting cases is quicker, and we briefly discuss this at the end of this appendix.

We recall that this structure is composed of four quadrants W_j each with solution w_j (see Figure 1), each of which has a different constant resistivity, ρ_j, with $j = 1, \ldots, 4$; the quadrants are numbered clockwise, with unity as the positive quadrant. In terms of complex velocity conjugate function $w(z) = \mathrm{d}\omega/\mathrm{d}z$ the boundary

conditions are that

$$\begin{array}{ll} \mathrm{Im}[i(\rho_1 w_1 - \rho_2 w_2)] = 0, & \mathrm{Im}[w_1 - w_2] = 0 \quad \text{on } 0 < x < \infty, \\ \mathrm{Im}[i(\rho_4 w_4 - \rho_3 w_3)] = 0, & \mathrm{Im}[w_4 - w_3] = 0 \quad \text{on } -\infty < x < 0, \\ \mathrm{Im}[i(w_4 - w_1)] = 0, & \mathrm{Im}[\rho_4 w_4 - \rho_1 w_1] = 0 \quad \text{on } 0 < y < \infty, \\ \mathrm{Im}[i(w_2 - w_3)] = 0, & \mathrm{Im}[\rho_2 w_2 - \rho_3 w_3] = 0 \quad \text{on } -\infty < y < 0. \end{array} \tag{A.1}$$

The solutions of this boundary value problem, $w_j(z)$, should have integrable singularities at $z = 0$, as should the function $w_j(1/z)$. To place this in a more malleable form we introduce the functions $u_j(z)$ for $j = 1, \ldots, 4$ as

$$u_1(z) = w_1(z), \quad u_2 = \overline{w_2(\overline{z})}, \quad u_3(z) = w_3(-z), \quad u_4 = \overline{w_4(-\overline{z})}, \tag{A.2}$$

which are defined and holomorphic in the positive quadrant W_1. Thus now we need only concentrate upon the first quadrant W_1. Using (A.2) we can rewrite boundary conditions (A.1) as follows:

$$\begin{array}{ll} \mathrm{Im}[i(\rho_1 u_1 - \rho_2 u_2)] = 0, & \mathrm{Im}[u_1 + u_2] = 0 \quad \text{on } 0 < x < \infty, \\ \mathrm{Im}[i(\rho_4 u_4 - \rho_3 u_3)] = 0, & \mathrm{Im}[u_4 + u_3] = 0 \quad \text{on } 0 < x < \infty, \\ \mathrm{Im}[i(u_4 - u_1)] = 0, & \mathrm{Im}[\rho_4 u_4 + \rho_1 u_1] = 0 \quad \text{on } 0 < y < \infty, \\ \mathrm{Im}[i(u_2 - u_3)] = 0, & \mathrm{Im}[\rho_2 u_2 + \rho_3 u_3] = 0 \quad \text{on } 0 < y < \infty. \end{array} \tag{A.3}$$

A matrix notation is now utilized such that

$$\mathrm{Im}[\mathbf{U}K_1] = 0, \; x > 0; \quad \mathrm{Im}[\mathbf{U}K_2] = 0, \; x < 0, \tag{A.4}$$

where $\mathbf{U}(\zeta)$ is a vector defined as

$$\mathbf{U}(\zeta) = \left[u_1(\sqrt{\zeta}), u_2(\sqrt{\zeta}), u_3(\sqrt{\zeta}), u_4(\sqrt{\zeta})\right] \tag{A.5}$$

in the upper half of the ζ plane, $\mathbb{C}^+$, and $K_{1,2}$ are the matrices

$$K_1 = \begin{pmatrix} \mathrm{i}\,\rho_1 & 1 & 0 & 0 \\ -\mathrm{i}\,\rho_2 & 1 & 0 & 0 \\ 0 & 0 & -\mathrm{i}\,\rho_3 & 1 \\ 0 & 0 & \mathrm{i}\,\rho_4 & 1 \end{pmatrix}, \quad K_2 = \begin{pmatrix} -\mathrm{i} & \rho_1 & 0 & 0 \\ 0 & 0 & \mathrm{i} & \rho_2 \\ 0 & 0 & -\mathrm{i} & \rho_3 \\ \mathrm{i} & \rho_4 & 0 & 0 \end{pmatrix}. \tag{A.6}$$

Due to (A.4) the vector-function

$$\mathbf{V}(\zeta) = \begin{cases} \mathbf{U}(\zeta)K_1 & \text{for} \quad \mathrm{Im}(\zeta) > 0, \\ \overline{\mathbf{U}(\overline{\zeta})K_1} & \text{for} \quad \mathrm{Im}(\zeta) < 0 \end{cases} \tag{A.7}$$

is the analytical continuation of the function $\mathbf{U}(\zeta)K_1$ into the lower half-plane across the positive part of the real axis. Thus, for $\zeta = \xi$, where ξ is real, we have $\mathbf{V}^+(\xi) = \mathbf{V}^-(\xi)$ for $\xi > 0$ and

$$\mathbf{V}^+(\xi) = \mathbf{V}^-(\xi)T \quad \text{for} \quad \xi < 0, \tag{A.8}$$

where

$$T = \overline{K}_1^{-1}\overline{K}_2 K_2^{-1} K_1. \tag{A.9}$$

In addition, the solution of the problem (A.8) has to satisfy a symmetry condition,

$$\overline{\mathbf{V}(\overline{\zeta})} \equiv \mathbf{V}(\zeta) \quad \forall \zeta \in \mathbb{C} \setminus (-\infty, 0], \tag{A.10}$$

due to the representation (A.7), and in the vicinity of origin in accordance with (A.5)

$$v_j(\zeta), v_j(1/\zeta) = \mathrm{o}(\sqrt{\zeta}) \tag{A.11}$$

for all components v_j of $\mathbf{V}$. It is clear that

$$K_1^{-1} = \begin{pmatrix} \frac{-\mathrm{i}}{\rho_1+\rho_2} & \frac{\mathrm{i}}{\rho_1+\rho_2} & 0 & 0 \\ \frac{\rho_2}{\rho_1+\rho_2} & \frac{\rho_1}{\rho_1+\rho_2} & 0 & 0 \\ 0 & 0 & \frac{\mathrm{i}}{\rho_3+\rho_4} & \frac{-\mathrm{i}}{\rho_3+\rho_4} \\ 0 & 0 & \frac{\rho_4}{\rho_3+\rho_4} & \frac{\rho_3}{\rho_3+\rho_4} \end{pmatrix},$$

$$K_2^{-1} = \begin{pmatrix} \frac{\mathrm{i}\,\rho_4}{\rho_1+\rho_4} & 0 & 0 & \frac{-\mathrm{i}\,\rho_1}{\rho_1+\rho_4} \\ \frac{1}{\rho_1+\rho_4} & 0 & 0 & \frac{1}{\rho_1+\rho_4} \\ 0 & \frac{-\mathrm{i}\,\rho_3}{\rho_2+\rho_3} & \frac{\mathrm{i}\,\rho_2}{\rho_2+\rho_3} & 0 \\ 0 & \frac{1}{\rho_2+\rho_3} & \frac{1}{\rho_2+\rho_3} & 0 \end{pmatrix}$$

and correspondingly

$$\overline{K_1^{-1}K_2} = \begin{pmatrix} \frac{-1}{\rho_1+\rho_2} & \frac{\mathrm{i}\,\rho_1}{\rho_1+\rho_2} & \frac{-1}{\rho_1+\rho_2} & \frac{-\mathrm{i}\,\rho_2}{\rho_1+\rho_2} \\ \frac{\mathrm{i}\,\rho_2}{\rho_1+\rho_2} & \frac{\rho_1\rho_2}{\rho_1+\rho_2} & \frac{-\mathrm{i}\,\rho_1}{\rho_1+\rho_2} & \frac{\rho_1\rho_2}{\rho_1+\rho_2} \\ \frac{1}{\rho_3+\rho_4} & \frac{\mathrm{i}\,\rho_4}{\rho_3+\rho_4} & \frac{1}{\rho_3+\rho_4} & \frac{-\mathrm{i}\,\rho_3}{\rho_3+\rho_4} \\ \frac{-\mathrm{i}\,\rho_3}{\rho_3+\rho_4} & \frac{\rho_3\rho_4}{\rho_3+\rho_4} & \frac{\mathrm{i}\,\rho_4}{\rho_3+\rho_4} & \frac{\rho_3\rho_4}{\rho_3+\rho_4} \end{pmatrix}.$$

Using this last representation, one finds the eigenvalues, μ, of the matrix (A.9) as the roots of

$$\det(\overline{K_1^{-1}K_2} - \mu K_1^{-1}K_2) = 0, \tag{A.12}$$

which is equivalent to $\det(T - \mu E) = 0$. It is not difficult to show that (A.12) has two coincident roots equal to -1 and two complex conjugated roots

$$\mu_{1,2} = \mathrm{e}^{\pm \mathrm{i}\,\pi\lambda} = \frac{\sigma_1\sigma_3 - \sigma_2^2}{\sigma_1\sigma_3 + \sigma_2^2} \pm 2\mathrm{i}\,|\sigma_2| \frac{\sqrt{\sigma_1\sigma_3}}{\sigma_1\sigma_3 + \sigma_2^2},$$

where $0 < \lambda \le 1$. Here

$$\sigma_1 = \rho_1 + \rho_2 + \rho_3 + \rho_4, \quad \sigma_2 = \rho_1\rho_3 - \rho_2\rho_4, \quad \sigma_3 = \rho_1\rho_2\rho_3 + \rho_1\rho_2\rho_4 + \rho_1\rho_3\rho_4 + \rho_2\rho_3\rho_4.$$

The earlier papers of Obnosov [26, 27] and Craster [7] primarily use a different notation involving a function Δ that is linked to the present notation via

$$\mu_{1,2} = \mathrm{e}^{\pm \mathrm{i}\,\pi\lambda} = 1 - 2\Delta^2 \pm \mathrm{i}\,2|\Delta|\sqrt{1-\Delta^2}, \tag{A.13}$$

where, in general,

$$\Delta^2 = \frac{\sigma_2^2}{\sigma_1\sigma_3 + \sigma_2^2} = \frac{(\rho_1\rho_3 - \rho_2\rho_4)^2}{(\rho_1+\rho_2)(\rho_2+\rho_3)(\rho_3+\rho_4)(\rho_4+\rho_1)}. \tag{A.14}$$

Let H be the matrix which brings matrix T into canonical Jordan form. Hence the function

$$\mathbf{V} = \mathbf{W}H$$

satisfies boundary condition

$$\mathbf{W}^+(\xi) = \mathbf{W}^-(\xi)T_0 \quad \text{for} \quad \xi < 0, \tag{A.15}$$

with T_0 as the diagonal matrix

$$T_0 = \begin{pmatrix} -1 & 0 & 0 & 0 \\ 0 & -1 & 0 & 0 \\ 0 & 0 & \mathrm{e}^{-\mathrm{i}\,\pi\lambda} & 0 \\ 0 & 0 & 0 & \mathrm{e}^{+\mathrm{i}\,\pi\lambda} \end{pmatrix}.$$

Finally, the general solution of the Riemann boundary value problem satisfying the condition (A.11) is

$$\mathbf{W} = (0, 0, c_1\zeta^{\lambda/2}, c_2\zeta^{-\lambda/2}), \tag{A.16}$$

where the branches of analytic functions above are fixed by the condition $|\arg\zeta| \le \pi$, and $c_{1,2}$, at this stage, are arbitrary complex parameters. Hence, the final solution of the problem (A.4) or, equivalently, (A.3) is a linear combination of two functions $\zeta^{\lambda/2}$ and $\zeta^{-\lambda/2}$. As these functions are linearly independent, the initial problem (A.1) has a particular solution of the form

$$w_{k1}(z) = A_k(\lambda)z^\lambda, \quad k = 1, \dots, 4, \tag{A.17}$$

with λ defined via (A.13) for some complex constants A_k; the second subscript on w_{k1} denotes that this is the first of two possible particular solutions, Additionally, it is clear that if $w_{k1}(z)$, $k = 1, \dots, 4$, is a solution of our problem (A.1), then so is $w_{k2}(z) = \overline{w_{k1}(1/\overline{z})} = \overline{A_k(\lambda)}z^{-\lambda}$, $k = 1, \dots, 4$. This occurs as the branch of the function z^λ is fixed by the condition $|\arg\zeta| < \pi$ and hence $\overline{1/\overline{z}^\lambda} = z^{-\lambda}$.

To summarize, the general solution of the problem (A.1) is

$$w_k(z) = C_1A_k(\lambda)z^\lambda + C_2\overline{A_k(\lambda)}z^{-\lambda}, \quad k = 1, \dots, 4, \tag{A.18}$$

with arbitrary real constants C_1, C_2.

However, it is also crucial to determine the parameters $A_k(\lambda)$ in (A.18). To achieve this aim we next use properties of the function $\nu(z) = z^\lambda$:

$$\overline{\nu(\overline{z})} \equiv \nu(z), \quad \nu(-z) = \begin{cases} \mathrm{e}^{-\mathrm{i}\,\pi\lambda}\nu(z), & \mathrm{Im}(z) > 0, \\ \mathrm{e}^{\mathrm{i}\,\pi\lambda}\nu(z), & \mathrm{Im}(z) < 0, \end{cases} \quad \overline{\nu(-\overline{z})} = \begin{cases} \mathrm{e}^{-\mathrm{i}\,\pi\lambda}\nu(z), & \mathrm{Im}(z) > 0, \\ \mathrm{e}^{\mathrm{i}\,\pi\lambda}\nu(z), & \mathrm{Im}(z) < 0. \end{cases}$$

In accordance with the properties of the vector in (A.5) with components defined via (A.2), (A.17) then holds with the representation

$$\mathbf{U}(\zeta) = \zeta^{\lambda/2}\left(A_1, \overline{A}_2, \mathrm{e}^{-\mathrm{i}\,\pi\lambda}A_3, \mathrm{e}^{-\mathrm{i}\,\pi\lambda}\overline{A}_4\right) = \zeta^{\lambda/2}\mathbf{U}_0. \tag{A.19}$$

Due to (A.4)

$$\mathrm{Im}[\mathbf{U}_0K_1] = 0, \quad \mathrm{Im}[\mathrm{e}^{\mathrm{i}\,\pi\lambda/2}\mathbf{U}_0K_2] = 0,$$

or equivalently

$$\begin{cases} \mathbf{U}_0K_1 - \overline{\mathbf{U}_0K_1} = 0, \\ \mathrm{e}^{\mathrm{i}\,\pi\lambda}\mathbf{U}_0K_2 - \overline{\mathbf{U}_0K_2} = 0. \end{cases}$$

Thence

$$\mathbf{U}_0\left(K_1\overline{K_1^{-1}K_2}K_2^{-1}-\mathrm{e}^{\mathrm{i}\,\pi l}E\right)=0 \quad \text{or} \quad \mathbf{U}_0K_1\left(T-\mathrm{e}^{\mathrm{i}\,\pi\lambda}E\right)K_1^{-1}=0.$$

Here matrix T has the form (A.9), and E is the unit matrix. As K_1 is a nonsingular matrix, we get

$$\left(T'-\mathrm{e}^{\mathrm{i}\,\pi\lambda}E\right)K_1'\mathbf{U}_0'=0, \tag{A.20}$$

where the prime denotes transposition. Thereby the column vector $\mathbf{V}_0'=K_1'\mathbf{U}_0'$ is the eigenvector of matrix T' corresponding to its eigenvalue $\mu_1=\exp[\mathrm{i}\,\pi\lambda]$. This is found after utilizing the symbolic manipulation packages in Mathematica [30] as

$$\mathbf{V}_0'=\left(\operatorname{sign}\sigma_2\sqrt{\sigma_3/\sigma_1},1,-\operatorname{sign}\sigma_2\sqrt{\sigma_3/\sigma_1},1\right)'.$$

Finally using (A.19) and the equality $\mathbf{U}_0=\mathbf{V}_0K_1^{-1}$, we find the $A_k(\lambda)$ as

$$\begin{aligned}
A_1(\lambda)&=\frac{\rho_2-\mathrm{i}\operatorname{sign}\sigma_2\sqrt{\sigma_3/\sigma_1}}{\rho_1+\rho_2}, & A_2(\lambda)&=\frac{\rho_1-\mathrm{i}\operatorname{sign}\sigma_2\sqrt{\sigma_3/\sigma_1}}{\rho_1+\rho_2},\\
A_3(\lambda)&=\mathrm{e}^{\mathrm{i}\,\pi\lambda}\left[\frac{\rho_4-\mathrm{i}\operatorname{sign}\sigma_2\sqrt{\sigma_3/\sigma_1}}{\rho_3+\rho_4}\right], & A_4(\lambda)&=\mathrm{e}^{-\mathrm{i}\,\pi\lambda}\left[\frac{\rho_3-\mathrm{i}\operatorname{sign}\sigma_2\sqrt{\sigma_3/\sigma_1}}{\rho_3+\rho_4}\right].
\end{aligned} \tag{A.21}$$

This is the closed-form solution to the joined quarter planes that we utilize in the text.

An alternative approach that is simpler for reduced cases of the above is to note that the problem is harmonic, and thus we expect solutions of the form $w_k=A_k(\lambda)z^\lambda$ $(k=1,\dots,4)$ and their conjugates. The aim is to identify λ as an eigenvalue and also the general form that the constants $A_k(\lambda)$ must take. Utilizing the boundary conditions in (A.1), we deduce a system of algebraic equations for the A_k together with an equation for λ as

$$4\Delta^2(1+\cos\lambda\pi)=(1-\cos 2\lambda\pi). \tag{A.22}$$

The solutions are $\cos\pi\lambda=1-2\Delta^2$ with Δ^2 given by (A.14); the $A_k(\lambda)$ also emerge as (A.21) but after considerably more algebra and also with the advantage of hindsight.

Appendix B. Useful integrals. These integrals are evaluated in [26] and are useful herein:

$$\frac{1}{h}\int_0^h\left(\tanh\frac{\pi iy}{2h}\right)^{\pm\lambda}dy=\frac{e^{\pm i\pi\lambda/2}}{\cos(\pi\lambda/2)}, \quad \frac{1}{l}\int_0^l\left(\tanh\frac{\pi x}{2h}\right)^{\pm\lambda}dx=1 \tag{B.1}$$

as $l\to\infty$,

$$\frac{1}{h}\int_0^h\zeta^{\pm\lambda}(iy)dy=\frac{e^{\pm i\pi\lambda/2}}{\sigma(1-m)\cos(\pi\lambda/2)}, \tag{B.2}$$

$$\frac{1}{l}\int_0^l\zeta^{\pm\lambda}(x)dx=\frac{1}{\sigma(m)\cos(\pi\lambda/2)}, \tag{B.3}$$

where ζ is the function defined in (5.1). We also use several other integrals that can be found in [26], in particular those associated with the dissipation. For purposes of brevity we refer the reader there for details.

Appendix C. Notation. Our complex notation is, at first sight, slightly different from the standard approach. This short appendix connects the two viewpoints.

The governing equations for the electric field $\mathbf{E}$ are

$$\nabla.(\sigma\mathbf{E}) = 0, \quad \nabla \times \mathbf{E} = 0, \tag{C.1}$$

with the conductivity, σ, constant in each homogeneous region. At an interface we have no jump in the tangential component of the field or the normal component of the current density leading to

$$[\![\sigma E_n]\!] = 0, \quad [\![E_t]\!] = 0, \tag{C.2}$$

where the $[\![\ ]\!]$ denote jumps in a quantity and the subscripts t, n denote tangential and normal components, that is, $\mathbf{E} = (E_n, E_t)$. As σ is constant in each cell we can define a potential ϕ such that $\mathbf{E} = -\nabla\phi$ and thus $\nabla^2\phi = 0$, so ϕ is harmonic, and this motivates the complex variable approach.

We choose to use a vector $\mathbf{w} = \sigma\mathbf{E}$, and thus

$$\nabla.\mathbf{w} = 0, \quad \nabla \times (\rho\mathbf{w}) = 0, \tag{C.3}$$

with ρ as the resistivity, constant in each cell. The vector $\mathbf{w}$ has interface conditions

$$[\![\rho w_t]\!] = 0, \quad [\![w_n]\!] = 0. \tag{C.4}$$

REFERENCES

[1] M. Abramowitz and I. A. Stegun, *Handbook of Mathematical Functions*, Dover, New York, 1969.

[2] V. L. Berdichevski, *The thermal conductivity of chess structures*, Vestnik Moskov. Univ. Ser. I Mat. Mekch., 40 (1985), pp. 56–63 (in Russian).

[3] L. Borcea, *Asymptotic analysis of quasi-static transport in high contrast conductive media*, SIAM J. Appl. Math., 59 (1998), pp. 597–635.

[4] L. Borcea and G. C. Papanicolaou, *Network approximation for transport properties of high contrast materials*, SIAM J. Appl. Math., 58 (1998), pp. 501–539.

[5] D. A. G. Bruggeman, *Berechnung verschiedener physikalischer Konstanten von heterogenen Substanzen*, Ann. Phys. Lpz., 24 (1935), pp. 636–679 (in German).

[6] H. Cheng and L. Greengard, *A method of images for the evaluation of electrostatic fields in systems of closely spaced conducting cylinders*, SIAM J. Appl. Math., 58 (1998), pp. 122–141.

[7] R. V. Craster, *On effective parameters for periodic checkerboard composites*, Proc. Roy. Soc. London Ser. A, 456 (2000), pp. 2741–2754.

[8] A. M. Dykhne, *Conductivity of a two-dimensional two-phase system*, Soviet Phys. JETP, 32 (1971), pp. 63–65.

[9] A. K. Gautesen, *The effective conductivity of a composite material with a periodic rectangular geometry*, SIAM J. Appl. Math., 48 (1988), pp. 393–404.

[10] J. Helsing, *Transport properties of two-dimensional tilings with corners*, Phys. Rev. B, 44 (1991), pp. 11677–11682.

[11] L. Hui and K. Bao, *Effective conductivity in a checkerboard geometry at high conductance ratio and high concentration*, Phys. Rev. B, 46 (1992), pp. 9209–9212.

[12] K. M. Jansons, *A general duality for nonlinear two-dimensional conduction*, IMA J. Appl. Math., 53, (1994), pp. 169–172.

[13] A. R. Kasimov and Y. V. Obnosov, *Groundwater flow in a medium with periodic inclusions*, Fluid Dynam., 30 (1995), pp. 758–766.

[14] J. B. Keller, *Conductivity of a medium containing a dense array of perfectly conducting spheres or cylinders or nonconducting cylinders*, J. Appl. Phys., 34 (1963), pp. 991–993.
[15] J. B. Keller, *A theorem on the conductivity of a composite medium*, J. Math. Phys., 5 (1964), pp. 548–549.
[16] J. B. Keller, *Effective conductivity of periodic composites composed of two very unequal conductors*, J. Math. Phys., 28 (1987), pp. 2516–2520.
[17] S. Kozlov and J. Vucans, *Explicit formula for effective thermoconductivity on the quadratic lattice structure*, C. R. Acad. Sci. Paris Sér. I Math., 314 (1992), pp. 281–286.
[18] D. F. Lawden, *Elliptic Functions and Applications*, Springer-Verlag, New York, 1989.
[19] F. K. Lehner, *Plane potential flows past doubly periodic arrays and their connection with effective transport properties*, J. Fluid Mech., 162 (1986), pp. 35–51.
[20] J. C. Maxwell, *A Treatise on Electricity and Magnetism*, Oxford University Press, London, 1904.
[21] K. S. Mendelson, *A theorem on the effective conductivity of a two-dimensional heterogeneous medium*, J. Appl. Phys., 46 (1975), pp. 4740–4741.
[22] G. W. Milton, *Proof of a conjecture on the conductivity of checkerboards*, J. Math. Phys., submitted.
[23] G. W. Milton, R. C. McPhedran, and D. R. McKenzie, *Transport properties of intersecting cylinders*, Appl. Phys., 25 (1981), pp. 23–30.
[24] V. V. Mityushev, *Transport properties of double-periodic arrays of circular cylinders*, Z. Angew. Math. Mech., 77 (1997), pp. 115–120.
[25] S. Mortola and S. Steffé, *A two-dimensional homogenization problem*, Atti Accad. Naz. Lincei Rend. Cl. Sci. Fis. Mat. Natur. (8), 78 (1985), pp. 77–82.
[26] Y. V. Obnosov, *Exact solution of a boundary-value problem for a rectangular checkerboard field*, Proc. Roy. Soc. London Ser. A, 452 (1996), pp. 2423–2442.
[27] Y. V. Obnosov, *Periodic heterogeneous structures: New explicit solutions and effective characteristics of refraction of an imposed field*, SIAM J. Appl. Math., 59 (1999), pp. 1267–1287.
[28] J. W. Rayleigh, *On the influence of obstacles arranged in rectangular order upon the properties of the medium*, Phil. Mag., 34 (1892), pp. 481–502.
[29] S. Torquato, *Random heterogeneous media: microstructure and improved bounds on effective properties*, Appl. Mech. Rev., 44 (1991), pp. 37–76.
[30] S. Wolfram, *Mathematica: A System for Doing Mathematics by Computer*, Addison-Wesley, Reading, MA, 1991.